Tilted pillar array fabrication by the combination of proton beam writing and soft lithography for microfluidic cell capture Part 2: Image sequence analysis based evaluation and biological application

G. Járvás[1,2], T. Varga[3], M. Szigeti[1,2], L. Hajba[1], P. Fürjes[4], I. Rajta[5], A. Guttman[1,2*]

[1]MTA-PE Translational Glycomics Group, MUKKI, University of Pannonia, Veszprém, Hungary

[2]Horváth Csaba Memorial Institute of Bioanalytical Research, University of Debrecen, Hungary

[3]Institute of Chemical and Process Engineering, University of Pannonia, Veszprém, Hungary

[4]Hungarian Academy of Sciences, Centre for Energy Research, Institute of Technical Physics and Materials Science, Budapest, Hungary

[5]MTA Atomki, Debrecen, Hungary

*Corresponding author; e-mail: a.guttman@northeastern.edu

Keywords: cell capture, proton beam writing, soft lithography, cell tracking, image sequence analysis

Abbreviations: **CFD** - Computational Fluid Dynamics, **MCCD** - Microfabricated Cell Capture Device, **PBS** - Phosphate Buffered Saline, **PBW** - Proton Beam Writing, **PDMS** - PolyDiMethylSiloxane

Total number of words: 3612

Abstract

Received: 06 29, 2017; Revised: 07 10, 2017; Accepted: 07 10, 2017

This article has been accepted for publication and undergone full peer review but has not been through the copyediting, typesetting, pagination and proofreading process, which may lead to differences between this version and the Version of Record. Please cite this article as doi: 10.1002/elps.201700268 .

As a continuation of our previously published work, this paper presents a detailed evaluation of a microfabricated cell capture device utilizing a doubly tilted micropillar array. The device was fabricated using a novel hybrid technology based on the combination of proton beam writing and conventional lithography techniques. Tilted pillars offer unique flow characteristics and support enhanced fluidic interaction for improved immuno-affinity based cell capture. The performance of the microdevice was evaluated by an image sequence analysis based in-house developed single cell tracking system. Individual cell tracking allowed in-depth analysis of the cell - chip surface interaction mechanism from hydrodynamic point of view. Simulation results were validated by using the hybrid device and the optimized surface functionalization procedure. Finally, the cell capture capability of this new generation microdevice was demonstrated by efficiently arresting cells from a HT29 cell-line suspension.

1 Introduction

Design, fabrication, integration and feasibility test results of a microfabricated cell capture device (MCCD) were published in the first part of this paper [1] highlighting the advantages of a novel combination of proton beam writing (PBW) [2] and conventional UV lithography. The resulting unique hybrid device had a small inner part of doubly tilted micropillar array for improved cell capture, fabricated by PBW, while the surrounding area of the chip was generated using UV lithography. This novel combination extended the potential of conventional microstructuring techniques generating high interest both from engineering and biological application points of views. The computational fluid dynamics (CFD) assisted chip design and the entire microfabrication process were demonstrated with some preliminary test results on flow characteristics [1].

Despite of the ever-growing interest in the development of innovative cell capture devices, this field is still in its early stage. Only a few studies focused on the in-depth evaluation of MCCDs, mainly

evaluating chip performance by calculating capture efficiency on the basis of selectivity and yield. This approach provided valuable data on the overall characteristics of the developed MCCDs but neither provided detailed information about the individual movement / trajectory of a given cell nor the cell - surface interaction. Kirby and coworkers carried out pioneering work to explore the mechanism of immuno-affinity based cell capture [3, 4] by studying the frequency of target/impurity cell – pillar collision. They concluded that capture performance in Hele-Shaw geometry was strongly dependent on the actual array layout. Similarly, the Toner group observed that cells flowing along streamlines in an ordered bed of posts have the same chance for adhering to a post surface of pillar-by-pillar [5, 6]. Therefore, they proposed a complex array where microposts were arranged in an equilateral triangular geometry. Dickson et al. developed an interesting MCCD, in which the diameter and spacing of posts were randomized to overcome the problem of low flow rates generally applied in microfluidic devices. In contrast, Viovy and his colleagues did not observe significant effect of shifting columns in the pillar array in case of their Ephesia device [7].

All of these studies significantly contributed to the better understanding of cell – solid phase interaction mechanisms, but the conclusions could not be directly applied to the tilted micropillars we have reported earlier. Therefore, as a continuation of our previous work, we evaluated the flow characteristics with the use of the developed flow distributor together with the doubly tilted micropillar array with special emphasis on their cell capture potential using a detailed image sequence analysis. The in-house developed analysis routine can assess the level of single cell behavior during the capture process. The microfluidic chip utilizing the special tilted micropillar component was used in all cell capture experiments. The major advantages of the hybrid device were the increased functional surface area and the enhanced dynamic behavior of the fluid in the capture chamber.

2 Theoretical considerations of single-cell tracking

One of the biggest challenges of computational fluid dynamics (CFD) generated models is the external validation part, which is even more difficult in case of microfabricated structures [8]. Particle tracing methods require a transparent chamber and colored tracer particles to determine the velocities in such a device [9]. The basic idea of this approach is the same as in particle image velocimetry methods, i.e., sufficiently small marker particles are illuminated and their pathway is recorded. However, image sequence processing methods can be used without laser excitation resulting in a much simpler setup and moderate experimental cost. By the utilization of image sequence analysis, even multiphase systems can be analyzed, assuming that of a transparent system and the recorded turbulent vortexes can be evaluated [10]. The concept of image sequence analysis is similar: intact visible particles are observed in recorded consequent images. Dedicated particles have to be identified frame by frame to identify the positions of the particles in each frame. The velocity of each cell can be calculated based on information about the detected lateral position of cells in consequent images and the corresponding time step.

In this study, cell trajectories were recorded using a digital camera - microscope objective assembly, which was placed above the flow through microchip device. The recorded image sequences were then analyzed by an in-house developed routine, performed in MATLAB 2015b environment utilizing functions form its Image Processing Toolbox. The motion analysis was based on direct comparison of the actual images against the reference images, i.e., the background. Recorded RGB images were converted to grayscale to reduce their complexity to help the cell tracking algorithm.

The first step of the detection procedure was the edge identification, where the Prewitt edge detection algorithm was applied with 0.02-0.08 threshold [11]. The applied optimal threshold value mainly depended on the image contrast, thus it was automatically adjusted for every image.

Comparison of the actual and background images resulted in coordinates of circle shape spots (built up from at least 50 pixels), which were collected as the actual positions of the cells in the microchip. A moving window approach was used to define the reference image, i.e., the background was handled as the average of 100 previous frames before the actual one. Utilization of the moving window technique was necessary since every successful cell capture event changed the background. The coordinates of each spot in every image and the detection time were collected during the analysis.

Reconstruction of the cell trajectories was based on the calculation of maximal cell movement using the coordinates of each observed cell. Negative differences (cells moving backwards) in coordinates were neglected. The cell identity criteria was set up as 40 pixels, meaning if the difference between two detected cells was less than the criteria then the cell was considered the same that was observed in the previous time step. The accepted coordinates were then acquired and the resulted trajectories evaluated.

3 Materials and Methods

3.1 Chemicals and Cell-culture solutions

If not noted otherwise, chemicals were purchased from Sigma-Aldrich (St. Louis, MO, USA). Colon cells from HT29 cell line (National Institute of Oncology, Budapest, Hungary) were cultured in 25 cm^2 tissue culture flasks. The cells were incubated at 37°C in carbon dioxide atmosphere and supplemented with RPMI-1640 culture media with 10% fetal bovine serum and 1% Penicillin-Streptomycin. In the flow-through experiments, cells were picked up with 0.5-0.2 % trypsin-EDTA solution and then resuspended in 1x phosphate buffered saline (PBS) with 1% NP-40 at 20,000 cells/ml concentration.

3.2 Surface functionalization of the microdevice

Our preliminary results suggested that antibody functionalization of the MCCD required oxygen plasma activated PDMS surface since chemical peroxidase treatment was not adequately effective. Oxygen plasma treatment on the other hand played a double role: 1) it sealed the patterned and precisely aligned microfluidic system onto a glass substrate, and 2) produced reactive Si-OH functional groups on the chip surface. Plasma activation of the PDMS surfaces was carried out in a dedicated plasma chamber (TerraUniversal Plasma-Preen, Fullerton, CA, USA) applying 200 W power for 2 min. The activated silanol groups were preserved by distilled water flooding until further processing. Functionalization of the microchips started by rinsing with 5% of 3-aminopropyltriethoxysilane (APTES) containing ethanol for 30 minutes. The APTES-coated surface was then activated with 2% aqueous glutaraldehyde solution (AppliChem Lifescience, Darmstadt, Germany) for 2 hours. Next, the activated surface was incubated overnight with recombinant protein G from Escherichia coli at a concentration of 50 $\mu g/ml^{-1}$ in PBS at 4ºC. The excess silanol groups were blocked by rinsing the channels with bovine serum albumin (BSA) solution (2 mg/ml^{-1} in PBS) and the system was incubated with the solution for 1 hour. Anti-EpCAM mouse antibody (Life Technologies, Carlsbad, CA, USA) at the concentration of 100 $\mu g/ml^{-1}$ in PBS was then added to the protein G layer and incubated for 1 hour. After these functionalization steps the MCCD was washed with PBS. Please note, all functionalization steps were conducted at 100 µl/h flow-rate.

3.3 Observation of single cell movement

The performance of the microfabricated device was evaluated by examining the flow pattern of HT29 colon cell suspension inside the MCCD, which was injected by a syringe pump (KD Scientific Inc., Holliston, USA) at 30 µl/h flow rate. Individual cell trajectories were monitored and recorded using a Nikon Eclipse TE200 (Nikon Instruments Inc., Tokyo, Japan) inverted microscope equipped

with a Hamamatsu C5810 cooled CCD camera (Hamamatsu Photonics K.K, Hamamatsu, Japan) as shown in Figure 1. Since the HT29 cells were clearly visible under normal light conditions, no staining was necessary. The acquired digital video footing was evaluated as described in Section 2.

3.4 Modeling

Details of the modeling approach were previously reported [1]. Briefly, the CAD model of the entire doubly tilted pillar array was imported in COMSOL Multiphysics (version 4.3.0.151, Stockholm, Sweden). The modeling was based on the laminar form of the Navier–Stokes transport equation, which was solved as a time-dependent problem. Flow conditions were set up with the same values used in the experimental work, i.e., velocity and pressure were defined at inlet and outlet boundaries. The applied mesh was tested for grid-size independency [8].

4. Results and discussion

4.1 Modeled cell trajectories

The calculated steady-state streamlines, as characteristic representation of the time-dependent solution, are shown in Figure 2, while additional modeling results were discussed earlier [1]. As one can observe, some of the streamlines end up at the pillars (especially in the lower middle section, depicted by arrows), suggesting that the fluid flow rate was below a certain specific velocity value, where most likely cell movements stopped. These regions can be considered as dead zones from fluid dynamics point of view. The negligible low ratio of the particular dead zones suggests that the design of the developed MCCD was close to the optimal configuration.

4.1 Cell tracking

Validation of the simulation results with experimental tests is a general requirement for all modeling based approaches [8]. Successful validation of the model consenting the use of simulation derived data was especially important in our case, where a novel and previously not investigated type of micropillar domain was modeled in 3D, including a complex system of flow obstacles and flow distributor as shown in Figure 3. Please note, in Figure 3 some of the pillars were apparently out of the embedding chip, which was due to the imperfect alignment. In such a microfluidic system, it was difficult to make direct flowrate and/or pressure measurements without disrupting the flow itself, thus reliable simulation data was of high importance. The modeled data were validated with an in-house developed cell tracking routine, based on image sequence analysis.

Figure 3 shows the processed image sequence demonstrating that most of the cells were detected, thus their trajectories could be calculated based on their movements. Around one third of the cells were not tracked with the developed routine most likely due to their pale cell walls and unexpected flow behavior. Blue lines, which represent the calculated trajectories of certain cells, were reconstructed from repeated observations (green circles) of the corresponding cells. Purple circles show the last positions of the cells in each pathways, where the tracking routine was still capable detecting them. Processing of complex biological samples, like cell suspensions, is a challenging technological problem even in case of cells from cell line cultures, since various coagulates often appear in the media as also shown in Figure 3. Clogged cell clusters (the big grey unstructured regions between the tilted array of micropillars) between the pillars may significantly affect flow characteristics. Hence, comparative measurements against the simulated results (which deal with an ideal case, lacking of any clogging) allows only qualitative evaluation. Therefore, in this study only sufficiently long trajectories were selected, which build up from at least 10 detected cell positions to

ensure clear comparison against the calculated pathways. 24 selected trajectories fulfilled this requirement, thus, were further investigated.

4.2 Evaluation of the flow distributor

A typical MCCD comprises an inlet/loading channel, a flow distributer, a functional part, and an outlet. One of the important aspects to the success of immune-affinity based microfluidic cell capture is the proper design for uniform flow velocity distribution while maximizing the flow rate [7, 12]. It was considered that combination of more channels in the sample load onto the micropillar array (functional part) may lead to more homogenous flow rate distribution. However, more channels on the same area result in smaller channel diameters, which raises the risk of clogging due to blood / cell coagulates. In order to overcome this limitation, the earlier developed inlet channel layout with a minimized footprint flow distributor [13] was utilized in the current work. Since commonly targeted rare-cells are very low abundant in human blood (typical concentration is in the order of 1-10 cell per mL of whole blood), the developed tilted micropillar array based chip was optimized to provide homogenous flow velocity distribution and consequently uniform spreading of cells with high cell capture efficiency. The flow distributor was modeled earlier by CFD [13] and experimentally verified during this study as an important part of the implementation of the proposed approach. Figure 4 shows the analysis of the resulted cell distribution visualizing the cell detection frequency in terms of the percentage of the total number of observations. The observed cell spreading was adequately homogenous in spite of the fact that the applied cell suspension was injected without any prior size based filtration, i.e., the sample contained spacious cell clusters and other components as discussed in section 4.1.

In addition to the excellent performance in forming uniform flow distribution, the developed flow distributor resulted in moderate pressure drop / flow resistance with minimized footprint.

4.3 Mechanism of cell capture

One of the most important advantages of immune-affinity based cell capture is its very high selectivity for the targeted cells due to the specificity of the antibody-antigen recognition. In this study, anti-EpCAM antibodies were used [5, 14], but the hybrid PDMS chip was suitable for any other types of capture agents. It is obvious that the overall cell capture efficiency is the sum of several factors such as the respective antibody and antigen density on the surface of the chip and the cells, the binding strength of the antibody-antigen interaction, the number of the potential binding sites, and the hydrodynamic characteristics of the cell – surface collusion including the exerted shear stress and contact time.

The developed image sequence based cell tracking method provided valuable information about the individual flow behavior of cells and capture mechanism. The velocity of the observed cells were derived from the recorded time dependent lateral positions (see section 4.1) and depicted in Figure 5.

Thorough inspection of the trajectories in Figure 5 revealed that some of the recorded paths (marked with A in Figure 5) were shifted towards the inclined side of the pillars. Most likely, this displacement effect was due to the asymmetric pressure and shear force distribution near the tilted micropillars [1]. Such a significant displacement effect proved to be especially beneficial from the capture efficiency point of view since cells, which were pushed towards the antibody covered pillar surface, were captured with higher probability. Interestingly, tracked cells did not slow down near the pillars (no color change visible on the trajectories), which was probably due to the similar inertia of the cells and the flowing media. Other cells flowing in the main stream were not affected by the intended lateral displacement, thus had similar apparent behavior like the cells processed in conventional cell capture devices [5].

5 Concluding remarks

In this paper a novel combination of proton beam writing and soft lithography techniques were applied to fabricate a microfabricated cell capture device. Development and application of an image sequence based individual cell tracking method was also reported. With the help of the developed routine, the flow characteristics of the previously developed flow distributor design, along with the revolutionary new, doubly tilted micropillar array was evaluated with special emphasis on its cell capture potential. The in-house developed analysis routine readily assessed the level of single cell behavior during the capture process. Fabrication of the hybrid microfluidic chip incorporated the advantages of proton beam writing and soft lithography and the resulted MCCD was used in all cell capture experiments. It was clearly demonstrated that the tilted pillars featured increased functional surface area and enhanced the fluid dynamics due to its lateral displacement effect.

Acknowledgements

The authors gratefully acknowledge the support of the Momentum (Lendulet) grant # 97101 of the Hungarian Academy of Sciences (MTA-PE Translational Glycomics) and the National Research, Development and Innovation Office (NKFIH) (K 116263) grants of the Hungarian Government. This work was also supported by the BIONANO_GINOP-2.3.2-15-2016-00017 project.

The authors have declared no conflict of interest.

References

[1] Rajta, I., Huszank, R., Szabo, A. T., Nagy, G. U., Szilasi, S., Furjes, P., Holczer, E., Fekete, Z., Jarvas, G., Szigeti, M., Hajba, L., Bodnar, J., Guttman, A., *Electrophoresis* 2016, *37*, 498-503.

[2] Huszank, R., Rajta, I., Cserháti, C., *Nuclear Instruments and Methods in Physics Research Section B: Beam Interactions with Materials and Atoms* 2015, *348*, 213-217.

[3] Smith, J. P., Lannin, T. B., Syed, Y., Santana, S. M., Kirby, B. J., *Biomedical microdevices* 2014, *16*, 143-151.

[4] Gleghorn, J. P., Pratt, E. D., Denning, D., Liu, H., Bander, N. H., Tagawa, S. T., Nanus, D. M., Giannakakou, P. A., Kirby, B. J., *Lab on a chip* 2010, *10*, 27-29.

[5] Nagrath, S., Sequist, L. V., Maheswaran, S., Bell, D. W., Irimia, D., Ulkus, L., Smith, M. R., Kwak, E. L., Digumarthy, S., Muzikansky, A., Ryan, P., Balis, U. J., Tompkins, R. G., Haber, D. A., Toner, M., *Nature* 2007, *450*, 1235-1239.

[6] Sequist, L. V., Nagrath, S., Toner, M., Haber, D. A., Lynch, T. J., *Journal of Thoracic Oncology* 2009, *4*, 281-283.

[7] Autebert, J., Coudert, B., Champ, J., Saias, L., Guneri, E. T., Lebofsky, R., Bidard, F. C., Pierga, J. Y., Farace, F., Descroix, S., Malaquin, L., Viovy, J. L., *Lab on a chip* 2015, *15*, 2090-2101.

[8] Jarvas, G., Guttman, A., *Trends in biotechnology* 2013, *31*, 696-703.

[9] Chenouard, N., Smal, I., de Chaumont, F., Maska, M., Sbalzarini, I. F., Gong, Y., Cardinale, J., Carthel, C., Coraluppi, S., Winter, M., Cohen, A. R., Godinez, W. J., Rohr, K., Kalaidzidis, Y., Liang, L., Duncan, J., Shen, H., Xu, Y., Magnusson, K. E. G., Jalden, J., Blau, H. M., Paul-Gilloteaux, P., Roudot,

P., Kervrann, C., Waharte, F., Tinevez, J.-Y., Shorte, S. L., Willemse, J., Celler, K., van Wezel, G. P., Dan, H.-W., Tsai, Y.-S., de Solorzano, C. O., Olivo-Marin, J.-C., Meijering, E., *Nat Meth* 2014, *11*, 281-289.

[10] Busciglio, A., Grisafi, F., Scargiali, F., Davi, M., Brucato, A., *Chemical Engineering Transactions* 2011, *24*, 1387-1392.

[11] Di, Y., Li, M. Y., Qiao, T., Lu, N., *International journal of ophthalmology* 2017, *10*, 336-342.

[12] Saias, L., Autebert, J., Malaquin, L., Viovy, J. L., *Lab on a chip* 2011, *11*, 822-832.

[13] Jarvas, G., Szigeti, M., Hajba, L., Furjes, P., Guttman, A., *Journal of chromatographic science* 2015, *53*, 411-416.

[14] Andree, K. C., van Dalum, G., Terstappen, L. W. M. M., *Molecular Oncology* 2016, *10*, 395-407.

Figure legends

Figure 1 Experimental setup for single cell tracing using a syringe pump (A), an inverted microscope (B) and a cooled CCD camera (C).

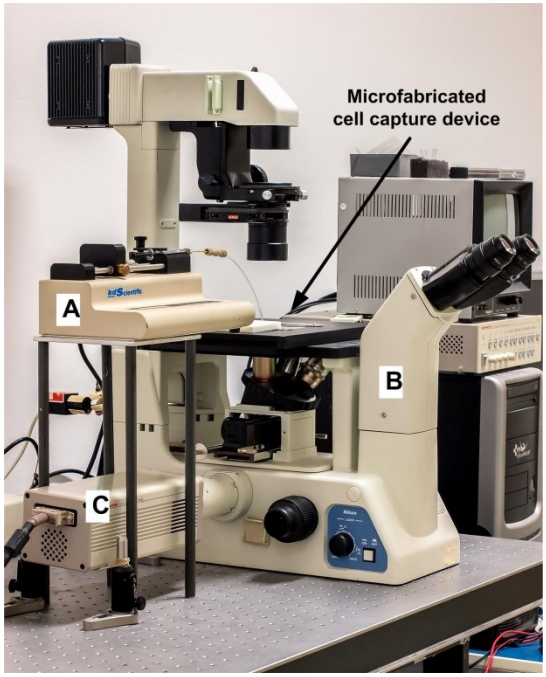

Figure 2 Calculated steady-state streamlines based on the developed model, expressed in term of fluid velocity [mm/s]. X and Y axes represent the geometrical scaling with μm unit.

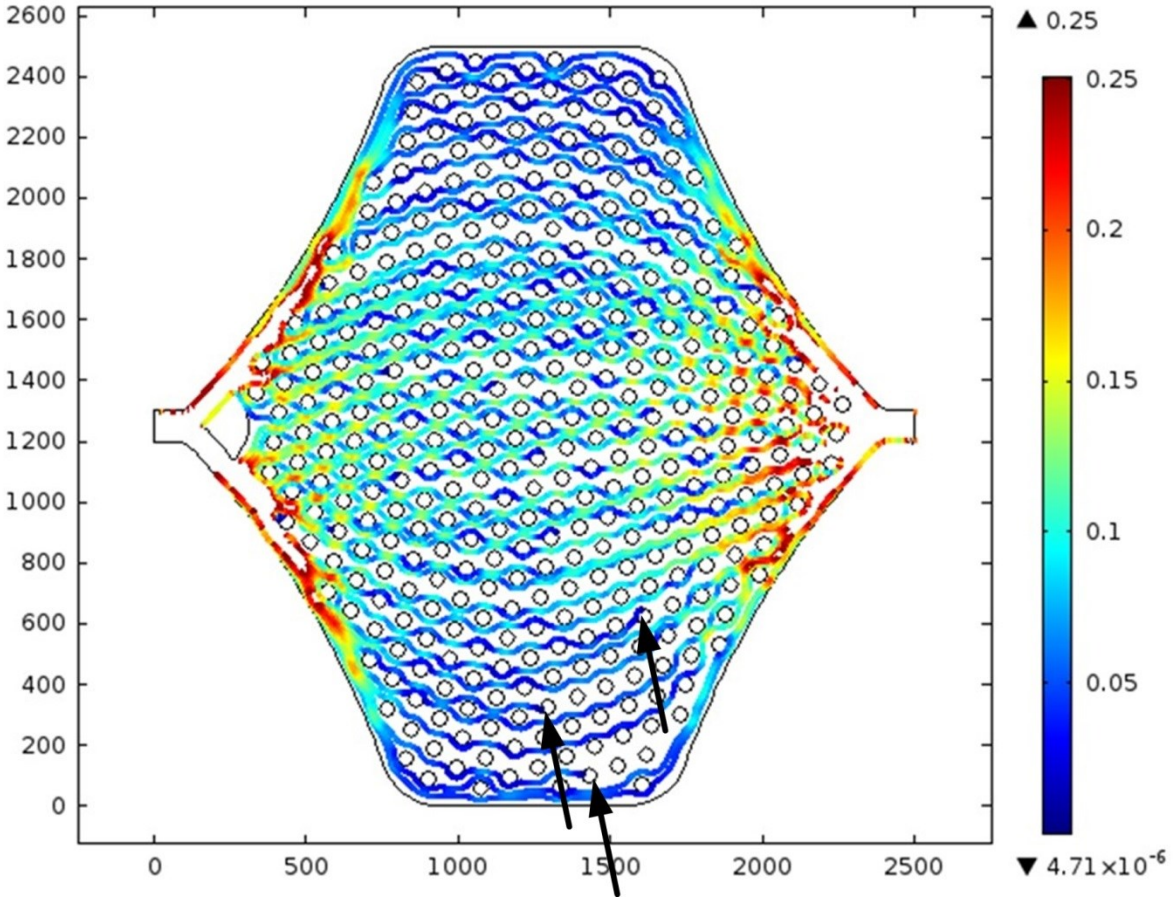

Figure 3 A representative screenshot from the acquired and processed image sequence video, showing the flow distributor (A), a cell cluster (B), which were clogged in the pillar array, and a free flowing cell cluster (C). Blue lines represent the observed cell trajectories reconstructed from the previous positions of the observed cells (green circles), while purple circles denote the ends of the tracked cell pathways.

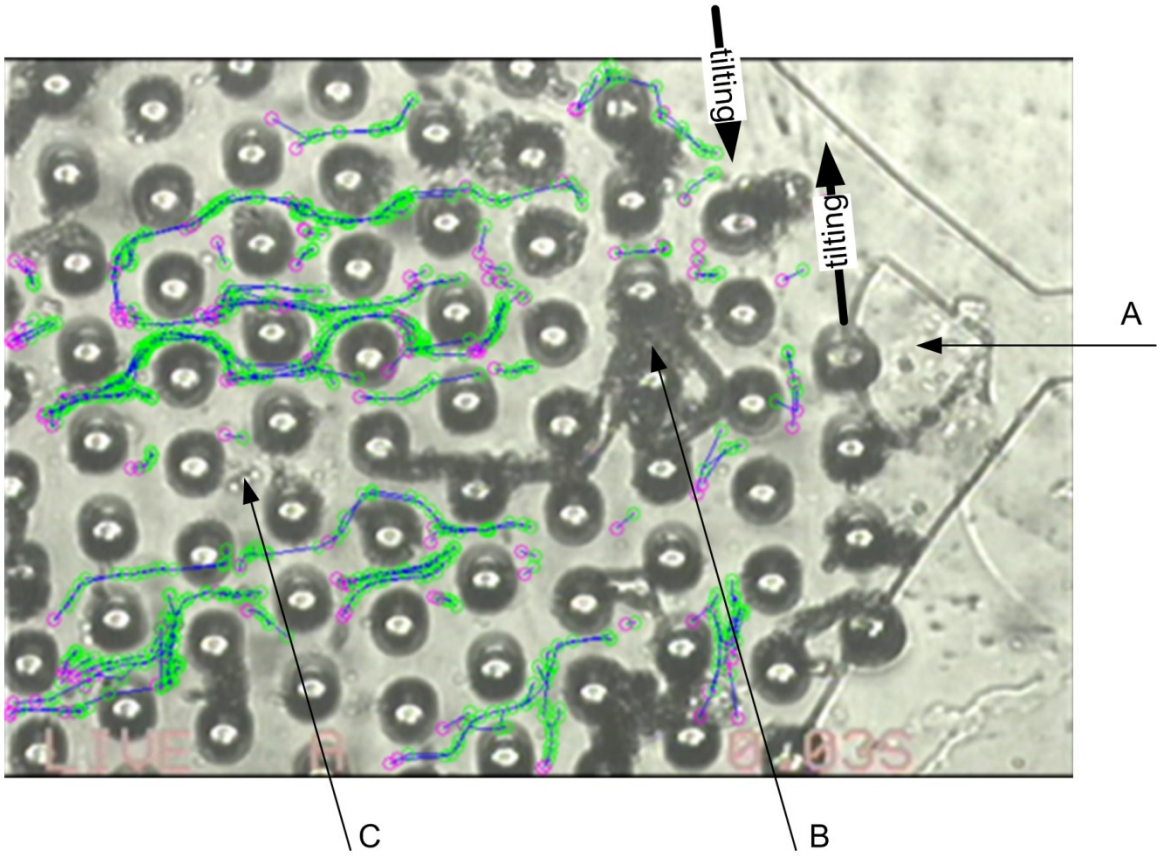

Figure 4 Heat-map visualization showing cell detection frequency in terms of the percentage of the total number of observations. Rectangles correspond to a certain volume of the pillar array, while their color indicates the cell observation frequency. Warmer colors depict higher likelihood of cell appearance. Notations: A - flow distributor, B - cell cluster clogs, C - free flowing cell cluster.

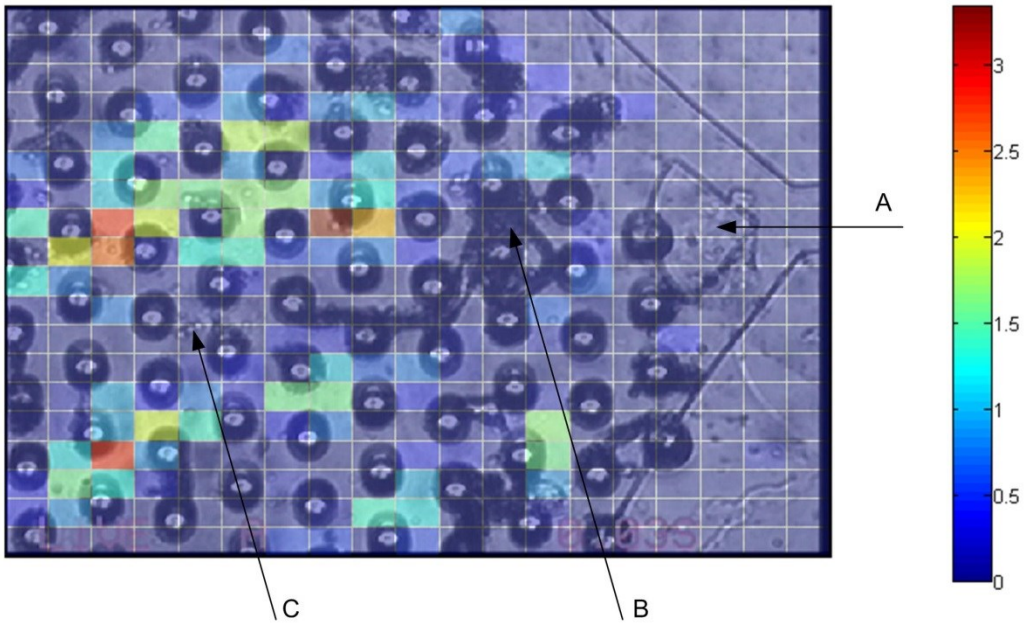

Figure 5 Calculated cell velocities at each point of the selected trajectories [mm/s].